DOI: ADD DOINUMBER HERE

Pre-conceptual staging trade-offs of reusable launch vehicles

Guillermo J. Dominguez Calabuig⋆ *and Jascha Wilken*†
Systemanalyse Raumtransport (SART), Deutsches Zentrum für Luft- und Raumfahrt (DLR)
Robert-Hooke-Straße 7, 28359 Bremen
⋆ Corresponding author , guillermo.dominguezcalabuig@dlr.de

Abstract

Reusable launch systems have revolutionized the space transportation industry during the last decade. The established success of Falcon 9 (SpaceX) played a pivotal role for many private companies and space agencies, pushing them to invest consistent resources in reusable launch vehicles (RLV) oriented on recovery for both main and upper stages. In this study, a novel pre-conceptual methodology for the sizing of reusable main stages based on optimal staging, structural index curves and rocket engine characteristics is introduced. The approach can serve to develop initial guesses and bounds for further detailed RLV sizing. It extends conventional launcher design methodologies, based on optimal staging with velocity budgets, to reusable trajectories with recovery hardware. This is used for a conceptual analysis of the suitability of design alternatives in terms of performance and parametric cost metrics and including different recovery solutions based on VTVL and VTHL rocket concepts. The study also explores the differences in using hydrogen, methane, propane, ammonia and kerosene as fuel. The results show the importance of modeling the recovery propellant and a sensitivity to the number of expected reuses for cost optimal designs differing from minimum take off mass solutions. Although it provides fast results which can be suitable to initialize the conceptual design of RLVs, its validity is limited as a consequence of the difficulty in conceptually modeling additional design parameters and their impact the vehicle trajectory and dry mass. Therefore, its results have to be carefully used within subsequent design phases, although it can be useful as an initialization strategy. Particularly, the velocity analysis discipline can produce initial guesses for detailed trajectory optimization, and the optimal staging routine for Multi-disciplinary Design Analysis and Optimization (MDAO) assessments. The performed trade-offs will be further complemented with future detailed studies on structural design and high fidelity MDAO.

Nomenclature

Acronyms

CER	Cost Estimating Relationship
DRL	Down Range Landing
ELV	Expendable Launch Vehicle
IAC	In Air Capturing
MDAO	Multi-disciplinary Design Analysis and Optimization
MER	Mass Estimating Relationship
RLV	Reusable Launch Vehicle
RTLS	Return To Launch Site
TSTO	Two Stages To Orbit
VTHL	Vertical Take-off Horizontal Landing
VTVL	Vertical Take-off Vertical Landing

Symbols

ΔV	Velocity budget	m/s
γ	Flight path angle	rad
Λ	Mass ratio	-
π	Payload ratio	-
θ	Pitch angle	rad
a_x	Axial load	g's
C_d	Drag coefficient	-
d	Diameter or Downrange	m
h	Altitude	m
I_{sp}	Specific Impulse	s
K	Mass based ballistic coefficient	kg/m^2
l	Length	m
m_d	Dry mass	Mg
m_i	Inert mass	Mg
m_L	Payload mass	Mg
m_s	Structural mass	Mg
m_T	Total mass	Mg
m_{es}	Mass of all engines	Mg
$m_{p,b}$	Propellant burned mass	Mg
$m_{p,res}$	Residual propellant mass	Mg
$m_{p,r}$	Recovery or deorbit propellant mass	Mg
$m_{p,ub}$	Propellant unburned mass	Mg

O/F	Oxidizer to fuel ratio	-	t	Time	s
q_c	Convective heat flux	W/m^2	T/W	Thrust to Weight	N
SI	Structural index	-	V	Speed	m/s

1. Introduction

Launch vehicle reusability is advancing significantly with Falcon 9 main stages being reused more than 10 times, leading to a new generation of space launch vehicles. Given the potential business case, many space actors are racing to develop cost effective design solutions, from Vertical Take Off Vertical landing (VTVL) ballistic launchers to horizontal landing concepts. This results in the need to consider a larger set of design criteria from the increased flight envelope, loads, recovery operations, maintenance and refurbishment aspects, leading to longer development cycles compared to expendable launch vehicles.

Among early conceptual design methodologies, the classical optimal staging methodology,[1–3] based on the Tsiolkovsky equation with multiple stages, presented an easy to implement design technique as a function of velocity budget to complete the mission ΔV, specific impulse I_{sp}, structural index SI and number of stages n_s. It therefore uses the Tsiolkovsky equation as:

$$\Delta V_a = \sum_{k=1}^{n} \Delta V_{a,k} = g_0 \sum_{k=1}^{n} I_{sp,e,k} \ln \Lambda_{a,k} \tag{1}$$

where ΔV_a is the ascent velocity budget, SI_k is the stage structural index and $I_{sp,e,k}$ the effective specific impulse

The resulting optimization problem becomes one of finding the optimal payload ratios, or velocity budget share, between the different stages, which can be used to minimize the cost function for a given payload mass or to maximize the payload ratio π_t. This method captures one of the largest technological trade-off for the design of rockets, the propellant choice and the number of stages. The former one results in a combination of specific impulse and structural index with different performance capabilities which can be assessed to check the mission feasibility.

The origins of this algorithm can be traced back to the beginning of rocket science, particularly to the Apollo era, when engineers faced the problem of how big each rocket stage should be in order to maximize its performance within their technological limits using the fundamentals of rocket flight. Previous studies optimized staging using an analytical Lagrange multiplier method for minimal take off weight and multiple stages and a fixed velocity budget.[2–4] It is mentioned in Hall et al[3] that this could incorporate velocity losses, while in Schurmann Ernest etal,[2] the gravity losses were estimated assuming a vertical flight with a flat earth approximation.[3] Gray et al[5] extended the method to a synthesized cost metric and a variable structural index with a non-linear dependency on propellant loading.

These alögorithms, however, had limits, highlighted by the difficulty of the classical optimal staging methodology to account for velocity losses with no direct dependency on the staging parameters.[6] This could lead to an over-sized second stage covering a larger mission budget share missing the resulting rise in velocity and pressure losses from starting the second stage at lower staging conditions. Different flight trajectory approximations were developed to estimate these losses,[7–10] although they increased the complexity of the analytical solution and incorporated limiting assumptions.

With the improvement of computational capabilities, it was possible to directly use optimization routines to solve the problem without the analytical Lagrange multipliers, as with a gradient based optimizer[11] or a global based genetic algorithm.[12–14] This allowed to lift certain assumptions, as constant structural index, specific impulse, and velocity budgets, to include additional optimization variables and detailed performance metrics.

Despite its simplicity, it is mentioned by[15] that the approach can lead to optimal gross lift of weights within 10-15% of the actual ones, and forms the basis of NASA's CONSIZ INTROS conceptual sizing codes. Nevertheless, although it allows for a simpler optimization, the performance of the launcher, or the required velocity budget to complete the mission, remains difficult to predict if no trajectory optimizations are performed.[6] More detailed automated approaches to find optimal solutions can be performed combining trajectory simulations and other disciplines such as propulsion, aerodynamics and structures in a Multidisciplinary Design Analysis and Optimization (MDAO) problem, which have been used for the design expendable launch vehicles[16] and reusable launchers. These can include relatively high fidelity disciplines for early conceptual design phases and can exploit the current computational resources efficiently with multi-dimensional gradient based and global algorithms. Nevertheless, gradient based approaches still suffers from the need of robust initial guesses for the design, while global heuristic based algorithms have slow convergence, need adequate problem bounds and still require refinement steps to converge to adequate solutions. It is therefore necessary to initialize these approaches with some robust initial guesses.

An approach to tackle this is to initialize by performing trajectory optimizations with simplified models and certain assumptions on the other vehicle architecture and technological choices. The simpler optimal staging methodology

can be used[17] with a fixed velocity budget to initialize trajectory optimizations and with other assumptions (thrust-to-weight ratios, axial accelerations at ignition and burnout), as used in CONSIZ INTROS.[15] Other studies[18,19] also used the simplified staging algorithm with trajectory optimizations using a coupled and decoupled approach for Expendables Launch Vehicles (ELV). There are recent studies extending the optimal sizing methodology to the design of reusable launch vehicles.[20,21] In both studies, the difficulty to include velocity losses arising from new mission profiles and the impact of design variables is observed. Although these could be mitigated with the inclusion of detailed trajectory assessments, it remains a challenge to maintain adequate fidelity while enabling fast conceptual trade-offs.

In this study, the optimal staging algorithm with fixed return velocity budgets presented in[21] is extended with a variable recovery velocity budget as a function of the first stage size based on a recent study for performance estimation of reusable launchers[22] and classical flight mechanics solutions.[23,24] A high-level Extended Design Structure Matrix (XDSM)[25] of the algorithm including staging, velocity budget estimation, and cost estimation disciplines is shown in Figure 1. The study then performs a trade off analysis of different Two Stages To Orbit (TSTO) launchers in terms of their optimality, take off mass and costs. The different configurations explored use expendable and reusable main stages with Vertical Take-off and Vertical Landing (VTVL) and Vertical Take-off Horizontal Landing (VTHL) technology, and are based on different propellant combinations using liquid hydrogen, methane, propane, kerosene or ammonia as fuel and liquid oxygen as oxidizer.

The later fuel, ammonia, was explored in this study as a potentially attractive fuel for reusability and for environmental impact mitigation.[26] Its highly efficient refrigerant properties can be an adequate option for active cooling systems as the rocket nozzle, its lower combustion temperatures may lead to a larger engine life, and it might be used with slight amount of hydrogen (stored separately or from cracking ammonia[a]) to increase its propulsion efficiency.[27] It was studied extensively in the past[28] and used successfully to power the rocket engine of the X-15 vehicle because of its rather benign handling requirements and adequate specific impulse. However, the slightly higher performance of hydrocarbon engines together with their availability and the need for highly efficient stages using hydrogen as fuel rendered it obsolete. Nevertheless, given its extensive use in agriculture and the current efforts to foster the hydrogen economy and green electrofuels, it might become widely available in the future and associated operating costs might reduce significantly.[27]

[a]As explored by Reaction Engines. "New UK joint venture for lightweight, modular ammonia crackers" Ammonia Energy Association, 2021. https://www.ammoniaenergy.org/articles/new-uk-joint-venture-for-lightweight-modular-ammonia-crackers/

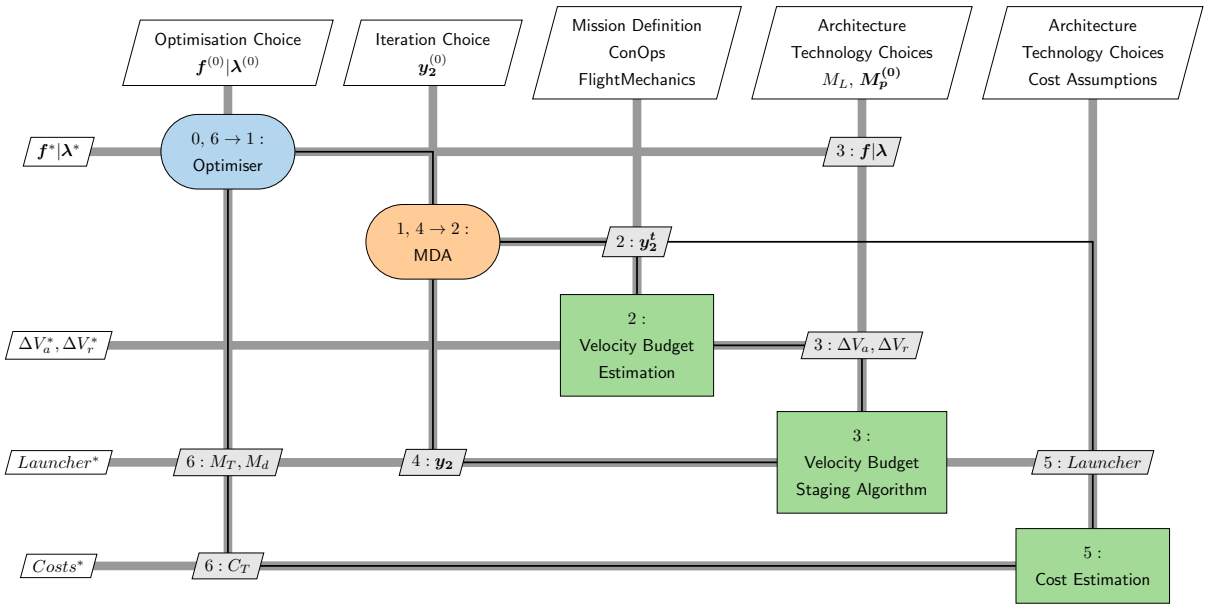

Figure 1: EXtended Design diagram (XDSM) of the simplified staging multi-disciplinary analysis and optimization methodology architecture. The parameter y_2 indicates all the output variables from the stage sizing algorithm which affect the velocity budget estimation presented in this paper, as the launcher surface reference area, ascent burn time and ballistic coefficient at stage separation

2. Definition of launcher and stages

In this simplified approach, the launch vehicle can be defined by breakdown of masses and other characteristics accounting for the propellant, structural masses, payload, initial engine thrust. In addition, each stage can be defined as an individual launcher described by the same breakdown. For a launcher with n stages, each stage $k \in \mathbb{Z}^n$ would have a total mass m_T^k of:

$$m_T^k = m_i^k + m_{p,b}^k + m_L^k \tag{2}$$

where m_i^k is the total inert mass, $m_{p,b}^k$ is the total burned propellant mass, and m_L^k is the stage payload mass composed of the total mass of the upper stage $m_L^k = m_T^{k+1}$.

The mass at the end of the burn is then given as:

$$m_b^k = m_T^k - m_{p,b}^k = m_i^k + m_L^k \tag{3}$$

The inert mass is then combined by a combination of unused propellant and all the remaining dry mass m_d^k (eg. propellant tanks, engines and other hardware). This can be decomposed on:

$$m_i^k = m_d^k + m_{p,ub}^k = m_s^k + m_{es}^k + m_{p,ub}^k \tag{4}$$

where m_s^k is the structural mass, $m_{es}^k = n_e\, m_e^k$ is the mass of all engines, with n_e being the number of engines and m_e^k being the mass of individual engines, and m_{p,ub_k} the unburned propellant mass defined as:

$$m_{p,ub}^k = m_{p,res}^k + m_{p,r}^k \tag{5}$$

which consists of the reserves and unusable propellant $m_{p,res}^k$ and the propellant mass for subsequent burns without the payload, as the recovery burns $m_{p,r}^k$, or de-orbit maneuvers. The total propellant mass m_p^k is then defined as:

$$m_p^k = m_{p,b}^k + m_{p,ub}^k \tag{6}$$

The reserve propellant can be assumed to be a fraction SF of the total propellant mass as

$$m_{p,res}^k = SF\, m_p^k \tag{7}$$

The total launcher Gross Take off Mass is defined by the first stage take off mass:

$$m_T = m_T^1 \tag{8}$$

whereas the total vehicle payload is provided by the payload mass of the final stage as:

$$m_L = m_L^n \tag{9}$$

The structural index, defined as a ratio of the rocket structures with respect to the total propellant can be defined as:

$$SI_k = \frac{m_d^k}{m_p^k} \tag{10}$$

Alternatively, it can also be defined as accounting for only structural masses as:

$$SI_{k,d} = \frac{m_s^k}{m_p^k} \tag{11}$$

The payload ratio can also be defined as:

$$\pi_k = \frac{m_L^k}{m_T^k} \tag{12}$$

with the total one given by a multiplication for all stages:

$$\pi_k = \prod_{k=1}^{n} \pi_k \tag{13}$$

On the other hand, the stage mass ratio can also be defined as:

$$\Lambda_{a,k} = \frac{m_T^k}{m_b^k} = \frac{1}{\epsilon_k(1-\pi_k) + \pi_k} = \frac{(S\,I_k + 1))}{S\,I_k(1-\pi_k) + (S\,I_k + 1)\,\pi_k} \tag{14}$$

and $\Lambda_{r,k} = \frac{m_i^k}{m_i^k - m_{p,r}^k}$ being the mass ratio for subsequent recovery operations.

The total velocity gained by this stage can then be obtained assuming constant specific impulse and the corresponding effective exhaust speed $c_{eff} = g_0\, I_{sp,eff}$ as:

$$\Delta V_{a,k} = g_0\, I_{sp,eff}^k \ln \Lambda_k = g_0\, I_{sp,eff}^k \ln \frac{(S\,I_k + 1)}{S\,I_k(1-\pi_k) + (S\,I_k + 1)\,\pi_k} \tag{15}$$

The total velocity supplied by the multi-stage rocket is then obtained as the sum of the individual velocity budgets:

$$\Delta V_a = \sum_{k=1}^{n} \Delta V_{a,k} \tag{16}$$

2.1 Launcher build-up depending on velocity budget

Launch vehicles perform complex trajectories to reach a desired orbit. These can be represented energetically by a total velocity budget (ΔV_a^r) that has to be supplied by the propulsion system while accounting for any encountered loss as a consequence of gravity, drag, or off-steering. Such budget has to be met by the velocity provided by the multistage rocket defined by Equation (16), as:

$$f : 0 = \Delta V_a^r - \sum_{k=1}^{n} \Delta V_{a,k} \tag{17}$$

Different procedures exist to evaluate the above relations and to determine the amount of velocity which each stage should provide. It can be seen that this selection can be chosen so that a vehicle achieves maximum performance π_T to a desired orbit, with a minimum take off mass m_T or maximum payload capability m_L, or different aspects can be weighted and it can be optimized for a minimum cost c_T. In this case, a fixed payload mass m_L to complete the mission was assumed and the launcher sized using a top-bottom approach.

One approach is to evaluate the vehicle performance given the velocity budget required by selecting the stage payload ratios π_k which satisfies Equation (17). This allows to build up the launcher by obtaining the ascent mass ratios:

$$\Lambda_{a,k} = \frac{(S\,I_k + 1)}{\Lambda_{r,k}\,(S\,I_k + S\,F)\,(1-\pi_k) + \pi_k\,(1 + S\,I_k)} \tag{18}$$

where $\Lambda_{r,k}$ for rocket propelled burns is computed as:

$$\Lambda_{r,k} = \exp\left(\frac{\Delta V_{r,k}}{g_0\, I_{sp,eff}^k}\right) \tag{19}$$

enabling the calculation of the propellant mass:

$$m_p^k = \frac{\left(1 - \Lambda_{a,k}^{-1}\right)}{\pi_k}\, m_{L,k} \tag{20}$$

which is typically solved with an indirect optimization method employing Lagrange multipliers for simple objective functions and $S\,I_k$.[4,20] Once these are computed, its possible to obtain the velocity supplied by the multi-stage rocket with Equation (16) which has to be enough to achieve the desired ΔV_a^r. This can be achieved by incorporating Equation (17) as an equality constraint of the problem.

A different approach assigns a fraction f_k of the total velocity budget required for each stage:[11]

$$\Delta V_k = f_k \Delta V_a^r \tag{21}$$

enabling through the complementary property to remove the upper stage fraction (or a different one) as:

$$f_n = 1 - \sum_{k=1}^{n-1} f_{\Delta V k}. \tag{22}$$

This can then be used to obtain the stage mass ratio using Equation (15) as:

$$\Lambda_{a,k} = \exp\left(\frac{\Delta V_{a,k}}{c_{eff,k}}\right) \tag{23}$$

and the payload ratio as:

$$\pi_k = \frac{SI_k + 1 - \Lambda_{a,k}\Lambda_{r,k}\,(SF + SI_k)}{\Lambda_{a,k}\,(SI_k + 1 - \Lambda_{r,k}\,(SF + SI_k))} \tag{24}$$

allowing for the calculation of the propellant mass using Equation (20).

Equations 18 or 24 can then be solved iteratively for total propellant mass m_p^k by using the dependency of the structural index on the propellant loading given in Section 3.1. The remaining properties can be determined through Equations (2) to (14).

3. Discipline models

The specific analysis disciplines within the optimal staging algorithm described in Section 2 are further described in the following sections

3.1 Mass budget and structural index

The structural index of launch vehicles is one of the main parameters determining its overall performance. It relates the amount of dry or unavailable mass that the launch vehicle carries with the propellant mass used to perform a specific burn, as given in Equation (10). The parameter decreases with total propellant mass as scaling up the different elements generally becomes structurally less complex and eases manufacturing. For example, the surface area to volume of the propellant tanks decreases with increasing size, lowering the amount of insulation needed. Additionally, it can also be dependent on the launcher aerothermodynamic and mechanical loads.

In this study, a parametric analysis was performed using SART's STSM and PMP tools for a launch vehicle with a length to diameter ratio of around 10 for the first stages, initial thrust to weight ratios of 1.4, an engine mass fraction of 20% of the total stage dry mass, staged combustion technology, different propellant combinations with oxygen as oxidizer and different fuels (hydrogen, methane, kerosene, propane and ammonia) with turbopump pressurization systems, and their corresponding recovery hardware. This procedure iterates through the STSM tool which uses semi-empirical methods for the dry mass estimation until the desired length to diameter and engine mass fraction is achieved. Within each call, PMP is executed which estimates the propellant tank weights depending on the propellant properties

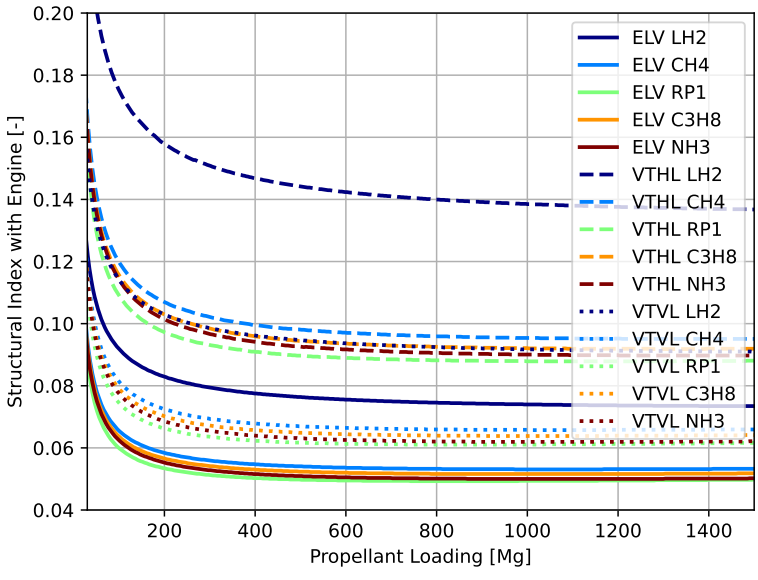

Figure 2: Structural index with engine for ELVs, VTHL, and VTVL launchers with hydrolox, methalox, propalox and kerolox propellant combinations

Table 1: Specific Impulse for the first and second stage, and oxidizer to fuel ratios (O/F) for the different propellant combinations assessed in this study, together with the area expansion ratios (ϵ). 16 MPa of chamber pressure are assumed. Values adapted from a previous study[29] using RPA and assuming staged combustion. Fuel storage temperature $T_{f,s}$ and an average propellant storage temperature $T_{p,s}$ based on mass (m) and calorific content at constant volume (C_v) assuming a LOX temperature of 90 K are also provided. Numbers in read indicate lowest performance in their category, while bold the opposite.

Fuel	Oxidizer	$T_{f,s}$ [K]	$T_{p,s}$ [K]		ρ_b [kg/m^3]	I_{sp} [s]		O/F	ϵ	
			m	C_v		Stage 1	Stage 2		Stage 1	Stage 2
Hydrogen	Oxygen	20	79	53	344	**415**	**460**	5.50	30	120
Methane	Oxygen	110	95	99	816	335	375	3.25	30	120
Kerosene	Oxygen	290	**144**	168	**1028**	325	365	2.70	30	120
Propane	Oxygen	230	133	139	915	331	371	2.90	30	120
Ammonia	Oxygen	238	135	**192**	893	310	345	1.40	30	120

using a simplified approach. The resulting structural index for ELVs with hydrogen and kerosene fuel was then calibrated with historical values for expendable launchers to reduce its prediction error which was seen to overestimate the structural index of hydrogen stages by 14% and underestimate that of kerosene by 8%, although high error bounds remained (MAPE of 23% and 26%, respectively). The resulting calibration factors were then linearly interpolated for methane, propane and ammonia based on their respective bulk stage densities ρ_b shown in Table 1. These were also used for VTVL and VTHL stages, with the resulting structural indexes shown in Figure 2. In addition, it also provided a reference value of the average fuselage cross section reference area. This is then interpolated based on the actual propellant mass inside the staging algorithm with a cubic interpolation algorithm.

It is seen how vehicles using kerosene as fuel achieve lower structural indexes through high bulk densities and reduced cryogenic insulation, followed by ammonia, propane and methane. Although these hydrolox stage require considerable insulation for their cryogenic hydrogen propellant tanks, the ratio of liquid oxygen used is significantly higher. The ammonia fueled stage is seen to achieve slightly lower structural indexes than the propane stage, even though it had an averaged bulk density slightly lower (Table 1). This could be explained by its low O/F ratio benefiting from the reduced density of fuel vs. oxidizer resulting in lighter tanks for the former and reduced cryogenic insulation. At the same time, it is seen how the requirements for recovery hardware as landing legs and fins for the VTVL vehicles and wings and landing gear for the VTHL vehicles leads to higher structural indexes, with VTHL requiring the largest dry mass. Nevertheless, high uncertainty remains in terms of the RLV stages structural index, which must be carefully in future work.

3.2 Propulsion system

The other important factor distinguishing different launch vehicle technologies and determining their performance is the specific impulse attained by the propulsion system. The averaged values used are based on staged combustion technology for the different propellant combinations. These, and their oxidizer to fuel ratios (O/F), are given in Table 1. For the first stage, an average between the sea level and the vacuum specific impulse was used. However, it should be noted that it may vary considerably depending on the altitude profiles during the different manoeuvres. This was accounted for heuristically depending on altitude location for the different manoeuvres.

3.3 Velocity budget estimation

The staging and optimization algorithm requires an estimate of the ascent and return velocity budget, or propellant mass, to size the launcher accordingly. Typically, highly detailed software for trajectory simulations and optimizations are used with careful analysis and engineering judgment. Nevertheless, at early design stages, this software is sometimes unavailable, less flexible or requires significant computational effort. In this study, a semi-empirical approach based on historical data and analytical solutions to powered and unpowered flight of launch and re-entry vehicles was used.

In past staging analysis studies, constant reusability budgets were employed.[21] Nevertheless this can vary considerably depending on the launch vehicle loading, orbit target, propellant type and its sizing characteristics. In this study, a semi-empirical approach was developed to estimate the stage separation conditions, combined with analytical flight mechanics solutions based on Keplerian trajectories and ballistic and lifting re-entry vehicles to estimate the corresponding velocity budget required for first stage reusability using the open source toolbox for solving and optimizing

complex systems of equations OpenMDAO.[30] On the other hand, the velocity budget required for deorbit operations can be assumed constant with a small impulsive of 300 m/s, although it can differ considerably depending on the target orbit.

Figure 3 shows an OpenMDAO design structure matrix (DSM) of the associated couplings for a VTVL case performing an RTLS maneuver. The underlying models are presented in the following subsections.

3.3.1 Ascent velocity budget

The ascent velocity required for different launchers to reach to specific orbit can be assumed similar as it slightly varies depending on the corresponding velocity losses. In this study, a constant ascent velocity budget for Low Earth Orbits (LEO) of 9.85 km/s was used.[11] Nevertheless, a sensitivity analysis to the resulting optimal solutions to various ascent velocity budgets was also performed, followed by an optimization with representative values for Geostationary Transfer Orbits (GTO) of 11.77 km/s.

3.3.2 Separation conditions

The computation of the stage separation conditions in the absence of detailed trajectory simulations is a major bottleneck for this approach. No analytical solution for the gravity turn manoeuvres with constant thrust exist. As a consequence, a semi-empirical approach was developed, similar to that employed in a previous study[22] with an assumed constant gravity loss.

Based on the estimate fo the first stage burn time at constant thrust magnitude and when throttling due to the maximum acceleration constraint, some gravity velocity losses can be assumed with an initial vertical flight of $t_p \approx 10s$, and a subsequent flight at constant flight path angle rate[24] as:

$$\Delta V_{g,loss} = \left(t_b\left(T/W, \Delta V_{a,1}, Isp, a_x\right) - t_p\right) g_0 \frac{\cos\gamma_s}{\pi/2 - \gamma_s} + t_p g_0 \tag{25}$$

The stage separation speed can then be computed:

$$V_s = \Delta V_{a,1} - \Delta V_{g,loss} \tag{26}$$

where $\Delta V_{a,1}$ is the ideal ascent velocity from the first stage. Note that the aerodynamic loss was neglected.

In addition to Equation (25) and Equation (26), a relationship between the flight path angle at stage separation γ_s, altitude h_s and downrange d_s is required. To obtain these, empirical fits were performed to past trajectories from SpaceX Falcon 9 flights obtained from raw webcast data reported in online sources[b]. Table 2 shows the accuracy of the selected regressions.

[b]Launch Dashboard API http://api.launchdashboard.space

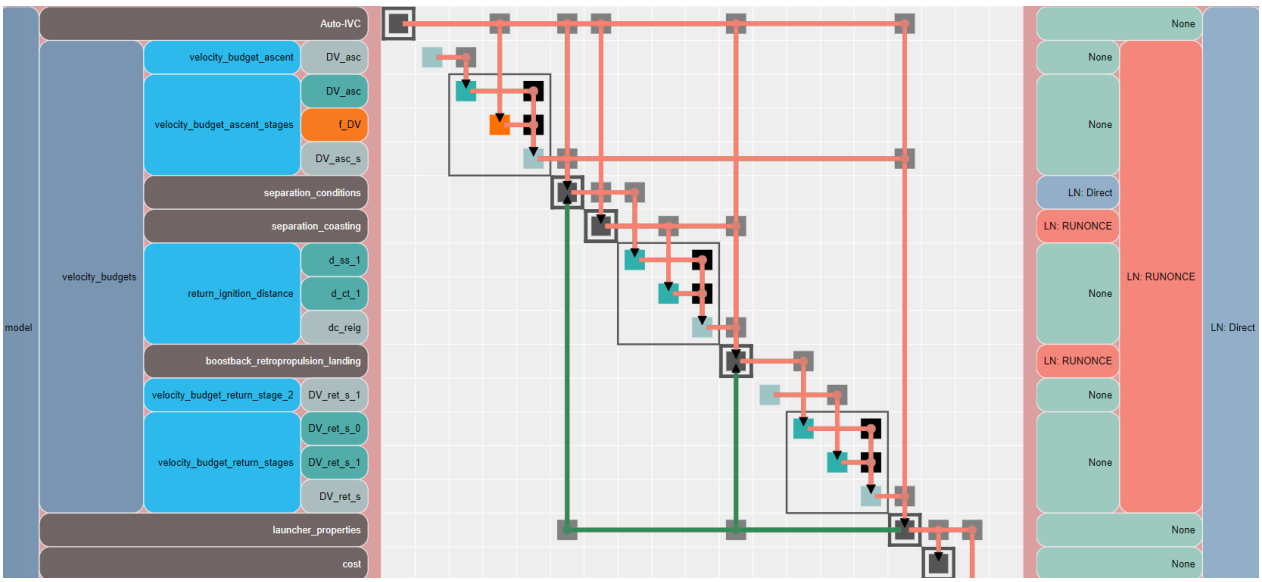

Figure 3: OpenMDAO design structure matrix (DSM) for the velocity budget based trajectory analysis of a VTVL launcher performing a RTLS manoeuvre

Table 2: Semi-empirical relations for stage separation conditions and related accuracy based on the adjusted coefficient of determination and mean average percentage error (MAPE). h_o represents the target orbit.

Variable	Equation	Input units	R^2_{adj}	MAPE
d_s	$0.0218129 V_s^2$	V_s [m/s]	0.90857	11.261 %
h_s	$1.30186981\, V_s^{0.387739930}\, h_o^{0.188295412}$ [km]	V_s [m/s], h_o [km]	0.48384	5.039 %
γ_s	$-0.75244033\, V_s^{0.80321655}\, h_o^{-0.34401691} + 90$ [deg]	V_s [m/s], h_o [km]	0.89826	8.8259 %

3.3.3 RTLS boostback manoeuvre

In order to return to launch site, a rocket propelled boostback maneuver can be performed. After separation, a coasting phase of around ≈ 10 seconds is assumed with a Keplerian motion, obtaining V_c, h_c, γ_c, d_c during which the right pitch angle is attained and sufficient clearance with the upper stage is obtained.

The launcher then ignites the engine and performs a boostback. It is seen from launch trajectories of SpaceX Falcon 9, that this typically occurs with a constant trust and a slightly negative constant pitch angle. To obtain analytical solutions for this problem, a constant gravity field and flat earth is assumed, and an initial load of approximately $(T/W)_{0,b} = 2.88$ and constant pitch of $\theta_b = 0$ is selected resulting in the equations:[24]

$$t_b = \frac{I_{sp}}{(T/W)_0}\left(1 - 1/\Lambda_b\right) \tag{27}$$

$$V_{x,b} = V_c \cos\gamma_c + \Delta V_b \cos\theta_b \tag{28}$$

$$V_{y,b} = V_c \sin\gamma_c + \Delta V_b \sin\theta_b - g_0 t_b \tag{29}$$

$$V_b = \sqrt{V_{x,b}^2 + V_{y,b}^2} \tag{30}$$

$$d_b = t_b V_c \cos\gamma_c + \frac{I_{sp}^2\, g_0}{(T/W)_0}\left(1 - \Lambda_b^{-1}\left(1 + \log\Lambda_b\right)\right)\cos\theta_b \tag{31}$$

$$h_b = t_b V_c \sin\gamma_c + \frac{I_{sp}^2\, g_0}{(T/W)_0}\left(1 - \Lambda_b^{-1}\left(1 + \log\Lambda_b\right)\right)\sin\theta_b - \frac{g_0\, t_b^2}{2} \tag{32}$$

where $\Lambda_b = \exp\left(\Delta V_b / c_{eff}\right)$.

It is then assumed that another coasting phase with Keplerian motion follows until the stage reaches an altitude h_r where heat fluxes become significant and the supersonic retro-propulsion maneuver is initiated. This is estimated assuming an exponential atmosphere and the Chapman equation for heat flux[31] at the nose with a maximum of $q_c = 20$ kW/m^2 and a fixed nose radius (assumed invariant of stage size) of $R_N = 0.5$, obtaining V_r, γ_r, d_r. The burn is performed until the required distance to the landing site reaches 0. This is computed by iterating ΔV_b until the following implicit equation is met:

$$f_b = 0 = d_s + d_c - d_b\left(\Delta V_b\right) - d_r\left(\Delta V_b\right) \tag{33}$$

3.3.4 Supersonic retro-propulsion maneuver

Once the maximum heat flux is reached, supersonic retro-propulsion begins with thrust angle opposing the velocity vector $\theta_r = -\gamma_r$, an initial thrust load of $(T/W)_{0,r} = 4.0$ from rough inspection of Falcon 9 trajectories, and an assumed ΔV_s. Equations (27) to (32) can be used by neglecting drag forces replacing the initial conditions (subscript c) with those corresponding to the maximum heat flux constraint (r), and the final conditions b with s. After V_s, h_s, γ_s, d_s are computed, it is assumed that the vehicle performs a quasi-vertical aerodynamic fall where gravity and aerodynamic forces remain at similar orders of magnitude. To compute this, the following equations were used:[23,32,33]

$$u = u_0 \exp\left(a\left(\sigma_0 - \sigma\right)\right) + a \exp\left(-a\sigma\right)\left(\mathrm{Expi}\left(a\sigma\right) - \mathrm{Expi}\left(a\sigma_0\right)\right) \tag{34}$$

$$a = 2 g_0 H_s / V_t^2 \tag{35}$$

$$V_t = \sqrt{2 g_0 K_a / \rho_0} \tag{36}$$

$$u = \left(V/V_t\right)^2 \tag{37}$$

$$\sigma = -\exp\left(-h/H_s\right) / \sin\gamma_s \tag{38}$$

where u is the dimensionless speed, σ the dimensionless altitude. Their initial values u_0, σ_0 being obtained using V_s, h_s in Equation (37) and Equation (38), respectively. K_s represents the stage mass based ballistic coefficient, which

can be computed from its value at stage separation K_s as $K_a = K_s\lambda_b^{-1}\lambda_s^{-1}$. This value can be obtained assuming a supersonic drag coefficient and with an estimate of the initial launch mass from the procedure described in Section 2. The maximum load experienced during this flight can be computed as:

$$\max a_x = -u_{max}\sigma_{max}\sin -\gamma_s \tag{39}$$

where u_{max} can be shown to be:

$$u_{max} = (\sigma_{max} - 1/a)^{-1} \tag{40}$$

Replacing Equation (40) in Equation (34), it is possible to obtain σ_{max} and compute n_x. Equation (39) is then used to obtain the maximum axial load, which is equated to 2.4 g's from inspection of Falcon 9 trajectories. The algorithm then iterates through the supersonic boost and the aerodynamic fall equations with ΔV_s until convergence.

3.3.5 Landing maneuver

The final landing maneuver is computed again assuming a constant thrust burn with an initial thrust to weight of $(T/W)_{0,l} = 2$ and a vertical burn with constant gravity and no drag forces. As the stage has a large ballistic coefficient, it is typically observed that the terminal velocity is never reached before landing, as opposed to what was assumed in previous studies.[22] The starting conditions are based on an aerodynamic fall equations Equations (34) to (38) by assuming a ballistic coefficient obtained similarly K_l as K_s but with a subsonic drag coefficient. A ΔV_l is assumed, obtaining V_f, h_f. The procedure then iterates on the assumed starting altitude h_l and ΔV_l until $V_f \approx 0$ and $h_f \approx 0$.

3.3.6 RTLS boostback maneuver with glide

For these manoeuvres, once the implicit Equation (33) is solved, it is assumed that the landing site is reached. Although this might lead to conservative results, as in reality range can be extended through the use of lift from the higher L/D of VTHL winged vehicles, the vehicle is on the other hand entering with high flight path angles from its suborbital arc, leading to high rate of descents until an equilibrium glide can be achieved, resulting in small range covered.

3.4 Cost estimation

Cost estimation becomes critical when considering the design of partially reusable TSTO launchers. Because of the additional reusability considerations, first stages tend to be larger and inefficient for providing the required ascent velocity budget when compared to typical architectures from expendable stages. As a consequence, if an optimized design is pursued in terms of minimal mass without factoring the advantages of the recovery and reuse of major structural components, it may result in low staging velocities with small first stages compared to the upper stages. To solve this, careful engineering judgment and an adequate cost estimation which can factor the masses of first and second stages adequately as well as considering the reusability cost effectiveness becomes critical.

In this study, a top down parametric approach using Cost Estimating Relationships (CERs) based on TRANSCOST[34] was performed adapting the open source cost estimation tool from[22] keeping the same quality factors for all propellants and assuming modern engines with no influence of propellant choice. Furthermore, recovery costs were estimated using correction factors for the TRANSCOST model based on bottom-up cost estimates for different recovery strategies.[35,36] For the cost estimation of stages with methane, propane and ammonia as fuel, no top down parametric approaches exist. A simplified surrogate approach was employed were the costs for a hydrogen and kerosene based stage CERs with the same mass were computed followed by a linear interpolation on predefined mass based average propellant storage temperatures $T_{p,s}$ provided in Table 1 (first sub-column m). This represents an assumed linearly increasing effort when handling cryogenic stages, although its validity has not been assessed. Table 1 also shows the calorific based averages (second sub-column) with a significant advantage for the ammonia fuel as a consequence of its lower O/F ratio and high specific heat value C_v which could indicate better cryogenic properties, although because of the extrapolation and uncertainty surrounding the ammonia stage it was not used for the surrogate model. It should also be noted that it might underestimate relative costs of hydrocarbon stages with respect to hydrogen stages, as the former ones were seen to have higher engine dry mass ratios.[29]

4. RLV architecture trade offs

The design methodology presented in the previous sections was used to perform a preliminary trade off between different configurations. A nominal mission to LEO was considered with a target payload requirement of 20 Mg, similar to the Falcon 9 and Ariane 6 capabilities. A typical fairing with a mass 13% of the LEO payload mass was

considered, and an inter-stage with 6% of the stage dry mass. In addition, reusable trajectories with maximum heat fluxes of 20 kW/m2 and 2.4 g's of axial acceleration were assumed. For cost assessment, the TRANSCOST model was assumed considering some default values for space agency based public development, manufacturing, operations and refurbishment, and an annual launch rate of 15. In terms of reusability, it is assumed that refurbishing stages and engines after launch could cost around 10% of producing a new one, and that these are reused up to 15 times, with 15 launches per year. The cost metric shown in the analysis and used for the optimization is the averaged launch efort in Workyears (Wyr) per launch. In addition, the ascent velocity fraction $f_{\Delta V,i} \in \mathbb{R}^{n-1}$ that each stage must attain was used as design variable to allow for a simpler uni-dimensional optimization problem for TSTO's problems as done by.[11] The results were also subjected to sensitivity assessments considering a GTO target orbit with 7 Mg as target payload, and the resulting optimal cost LEO configurations were also assessed for different orbits with various velocity budgets.

4.1 Expendable launchers

A preliminary assessment for expendable launchers was performed based on the structural indexes and specific impulses provided in Section 3. Figure 4 shows the total mass for the launch vehicles as a fraction of the first stage ascent velocity fraction. The asterix in the figure show the minimal effort configuration with a slightly larger first stage

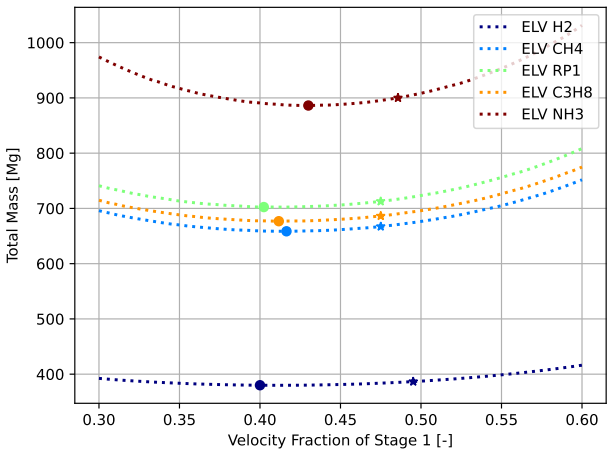

Figure 4: Total mass vs. first stage ascent velocity fraction for kerosene, methane and hydrogen expendable launch vehicles. The circled dot (•) shows the minimal total mass configuration, while the asterix (∗) the minimal effort configuration.

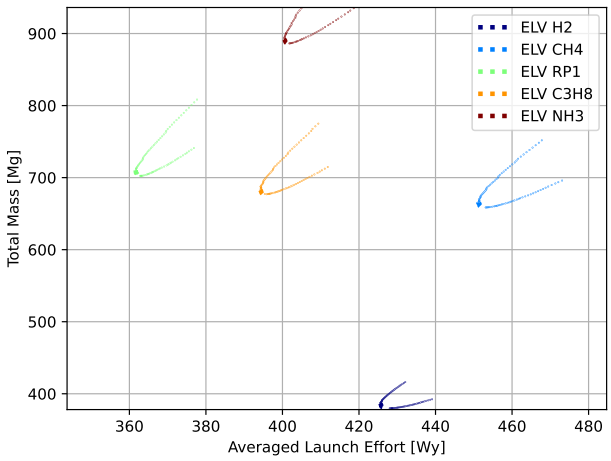

Figure 5: Total take off mass vs launch effort for kerosene, methane and hydrogen TSTO expendable launch vehicles.

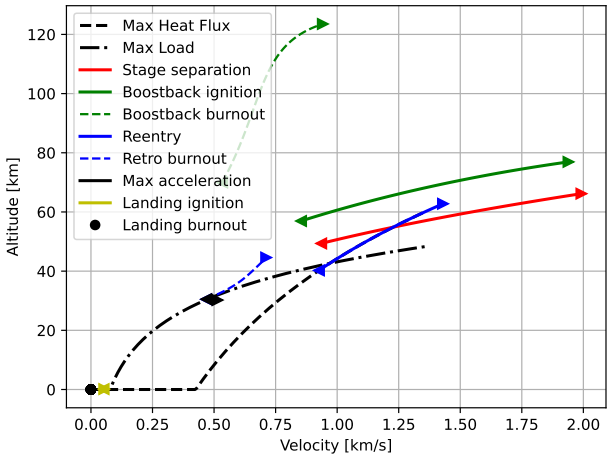

Figure 6: Entry corridor based on staging velocities for hydrogen based RTLS VTVL TSTO vehicle.

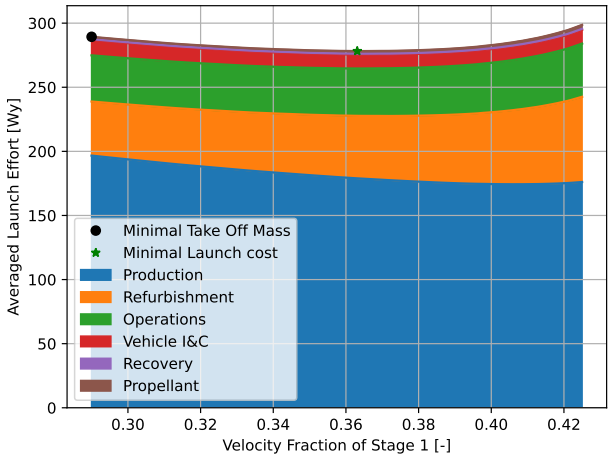

Figure 7: Launch cost breakdown for hydrogen based RTLS VTVL TSTO vehicle.

compared to the minimum take off mass condition as its costs per stage dry mass become smaller for larger propellant masses. A slight "wobbling" in the results can be observed, as a consequence of the numerical solvers which was traced back to discontinuities and interpolation from the structural index curves. A Pareto plot of the optimal configurations in terms of total mass and launch costs is shown in Figure 5. The figures show that although hydrogen based launch vehicles lead to highly efficient launchers with minimum total masses, the estimated launch effort remains higher than kerosene configurations as a consequence of the estimated higher complexity, although still lower than the cryogenic methane fueled stages. It can also be seen how propane and ammonia fueled launchers perform adequately in terms of estimated launch effort although this latest one has the highest total mass because of its reduced specific impulse resulting in higher propellant mass.

4.2 VTVL launchers

The VTVL launchers considered in this study use a reusable ballistic main stage with powered landing capabilities combined with an expendable second stage. It performs a flight profile based on a tossback maneuver to boost back to the landing site, combined with a steep suborbital re-entry followed by a retro propulsion to reduce aerodynamic

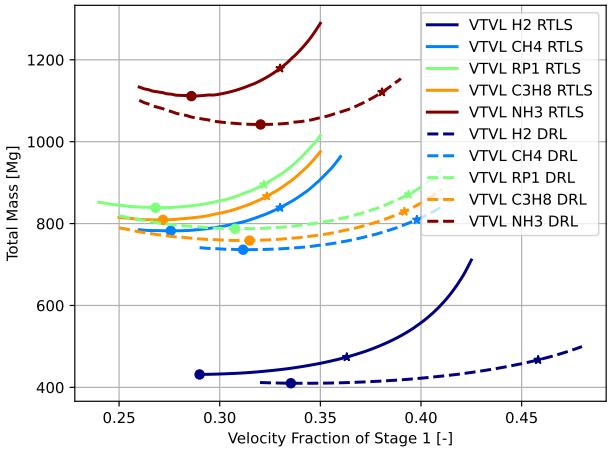

Figure 8: Total mass vs. first stage ascent velocity fraction for kerosene, methane and hydrogen VTVL TSTO launch vehicles targeting LEO. The circled dot (•) shows the minimal total mass configuration, while the asterix (∗) the minimal effort configuration.

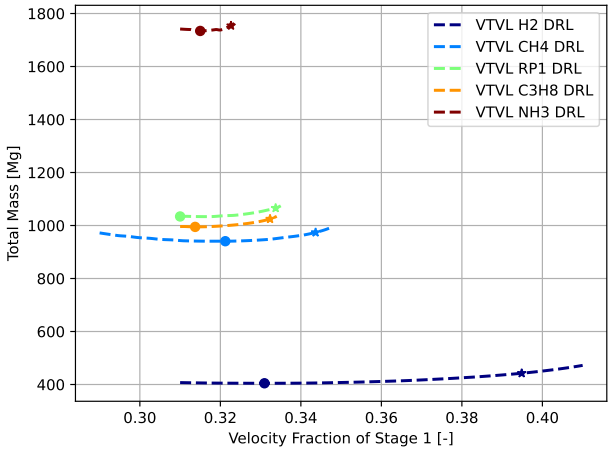

Figure 9: Total mass vs. first stage ascent velocity fraction for kerosene, methane and hydrogen VTVL TSTO launch vehicles targeting GTO. The circled dot (•) shows the minimal total mass configuration, while the asterix (∗) the minimal effort configuration.

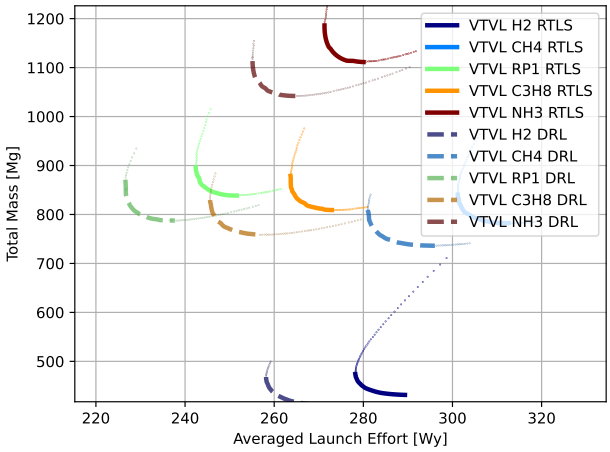

Figure 10: Total take-off mass vs. launch costs for kerosene, methane and hydrogen VTVL TSTO vehicles targeting LEO.

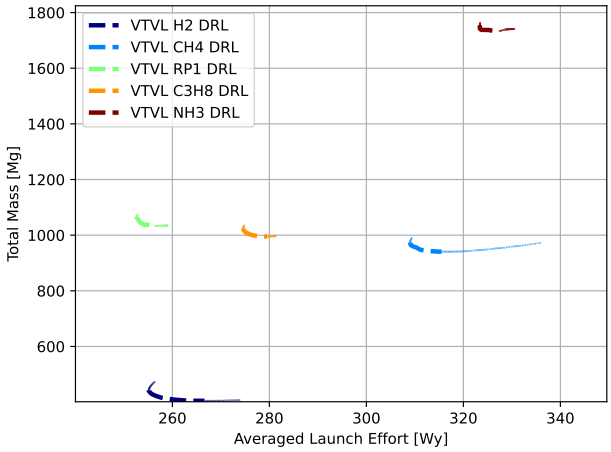

Figure 11: Total take-off mass vs. launch costs for kerosene, methane and hydrogen VTVL TSTO vehicles targeting GTO.

Table 3: Results for VTVL launchers with cost optimal staging targeting LEO

Propellant		Hydrolox		Methalox		Kerolox		Propalox		Ammolox	
Recovery Type		RTLS	DRL	RTLS	DRL	RTLS	DRL	RTLS	DRL	RTLS	DRL
Stage 1	m_T [Mg]	335	364	614	638	654	692	631	652	894	897
	m_d [Mg]	30	32	38	40	38	40	38	39	52	52
	$m_{p,a}$ [Mg]	277	313	527	564	564	613	542	577	774	794
	$m_{p,r}$ [Mg]	25	15	42	29	45	32	45	29	59	42
	SI [-]	0.10	0.10	0.07	0.07	0.06	0.06	0.06	0.06	0.06	0.06
	l [m]	59	61	55	56	52	53	53	54	61	61
	ΔV_a [km/s]	3.58	4.51	3.25	3.92	3.17	3.88	3.19	3.86	3.25	3.75
	ΔV_r [km/s]	2.19	1.37	2.13	1.52	2.18	1.61	2.19	1.54	1.99	1.52
	$f_{\Delta V}$ [-]	0.36	0.46	0.33	0.40	0.32	0.39	0.32	0.39	0.33	0.38
	d_{drl} [km]		546		585		610		588		573
Stage 2	m_T [Mg]	114	79	200	146	217	154	210	152	259	198
	m_d [Mg]	10	7	11	8	11	8	11	9	13	10
	$m_{p,a}$ [Mg]	103	70	186	135	202	143	196	141	242	184
	$m_{p,r}$ [Mg]	1	1	1	1	1	1	1	1	2	1
	SI [-]	0.09	0.10	0.06	0.06	0.05	0.06	0.06	0.06	0.05	0.06
	l [m]	29	22	26	21	25	20	26	21	27	22
	ΔV_a [km/s]	6.27	5.34	6.60	5.93	6.68	5.97	6.66	5.99	6.60	6.10
	ΔV_d [km/s]	0.30	0.30	0.30	0.30	0.30	0.30	0.30	0.30	0.30	0.30
Launcher	m_T [Mg]	474	467	839	809	895	871	867	829	1179	1121
	$m_{L,ELV}$ [Mg]	25	24	26	24	26	25	26	24	27	25
	C_T [Wyr]	278	258	301	281	242	227	264	246	271	255
	l [m]	100	94	93	88	89	84	91	86	99	94
	d [m]	5.9	6.1	5.5	5.6	5.2	5.3	5.3	5.4	6.1	6.1

heating, a ballistic fall in denser parts of the atmosphere and a landing burn at adequate deceleration speeds. It can also land downrange in a floating barge or in another suitable location which benefits from avoiding the expensive tossback maneuver, which becomes infeasible for large payloads and demanding missions with large separation speeds. In this missions, considerable amounts of propellants are used combined with large burn times and numerous re-ignition cycles. Table 3 presents some results for the minimal effort configurations targeting LEO.

For this case, it is seen how the staging considerations become critical for the estimation of the return propellant mass fraction. In Figure 6, it is seen how the ideal velocity fraction difference results in significantly different toss-

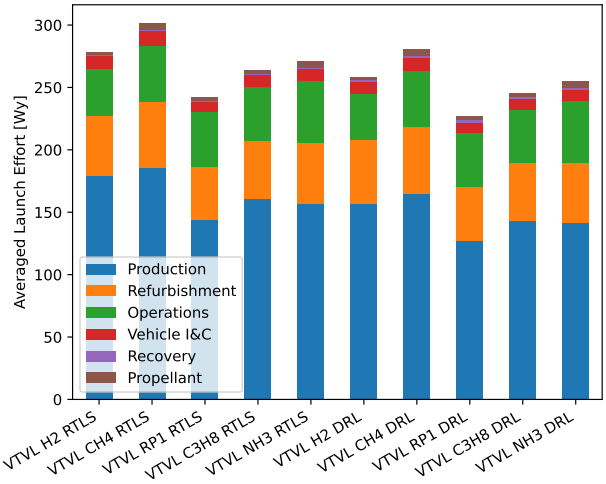

Figure 12: Launch cost effort breakdown for kerosene, methane and hydrogen VTVL TSTO launch vehicles.

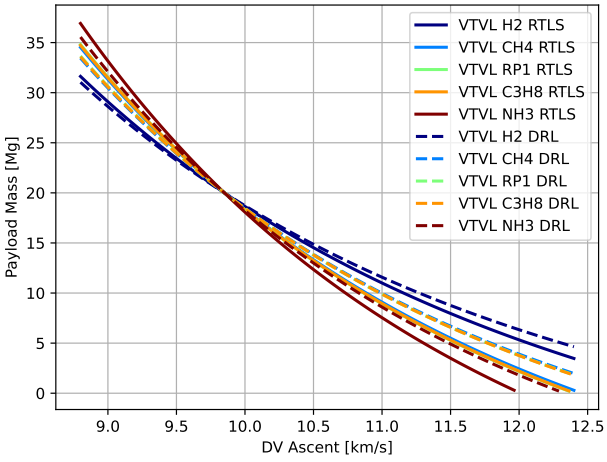

Figure 13: Payload performance for different ascent velocity budgets for hydrogen, methane and kerosene TSTO VTVL vehicles.

back manoeuvres with low burnout altitudes at low staging values. An opposite trend can be seen for the altitude of maximum aerodynamic loads after the supersonic burn, and for the landing burn starting conditions. It should be noted that the stage separation speeds for low velocity fractions are outside the range of validity of the semi-empirical approximation performed and might be underestimating recovery velocity budgets. It is recommended use data from more launchers or detailed trajectory optimizations to further refine the model.

In Figure 8, the stage total mass versus the total propulsive ascent velocity fraction of the first stage is shown, showing considerable differences between the minimal take off mass staging possibility with respect to the minimal launch costs one. This difference is explained by the large amounts of propellants needed for the recovery operations, which leads to high inert masses during ascent for the first stage, and an attempt by the optimal staging algorithm to compensate with bigger second stages. Nevertheless, when reusability considerations are introduced, the cost effectiveness from recovering and reusing the first stage leads to solutions with larger first stages with bigger ascent velocity budgets and stage separation conditions, even though recovery propellant amounts increase. The small contribution from the propellant can be also seen in Figure 7 and Figure 12 for the other configurations. In addition, Figure 8 also shows how launchers designed for RTLS manoeuvres require larger total masses in order to deliver the same amount of payload compared to DRL launchers. In addition, similar differences in staging propulsive velocity budget fraction is seen as for the previously described hydrogen-based launcher. The hydrocarbon and ammonia launchers show larger total take off masses compared to the hydrogen one as a consequence of the large propellant amounts necessary to complete the mission.

A comparison in terms of costs and take off masses for the different configurations is shown in Figure 10 for LEO and in Figure 11 for GTO. Here, a slight advantage for kerosene configurations compared to hydrogen-based launcher is seen in terms of estimated costs (although reduced for GTO), while methane shows a higher required effort. For LEO, is seen how propane and ammonia configuration show attractive characteristics in terms of launch effort, similar to hydrogen, while this difference significantly changes for GTO, with ammonia performing worse than methane. Nevertheless, as seen in Figure 13, the hydrogen-based configuration could attain significantly higher payload masses for missions requiring larger velocity budgets.

4.3 VTHL launchers

VTHL vehicles use wings to perform smoother suborbital re-entries after main stage separation. The launcher can then land downrange at suitable landing sites or it can be captured by an airplane or helicopter for retrieval to the launch complex and immediate refurbishment. In addition to this, the launcher could also employ its rocket engine to perform a tossback burn towards the launch site soon after separation or after a downrange entry as a 'hop' maneuver. In this study, an early return burn at stage separation was considered for RTLS approaches with a 2.8 initial thrust load constant thrust boost. Nevertheless, because of the lack of supersonic deceleration and steep entry flight path angles, considerable heat fluxes and aerodynamic loads may be expected after entry depending on its ballistic coefficient,

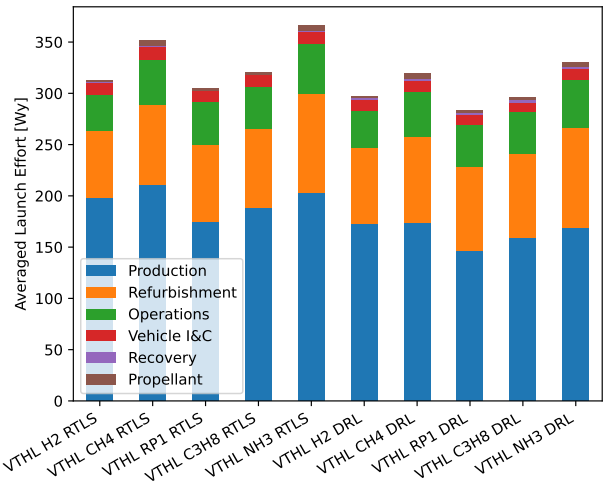

Figure 14: Launch cost effort breakdown for kerosene, methane and hydrogen VTHL TSTO launch vehicles targeting LEO.

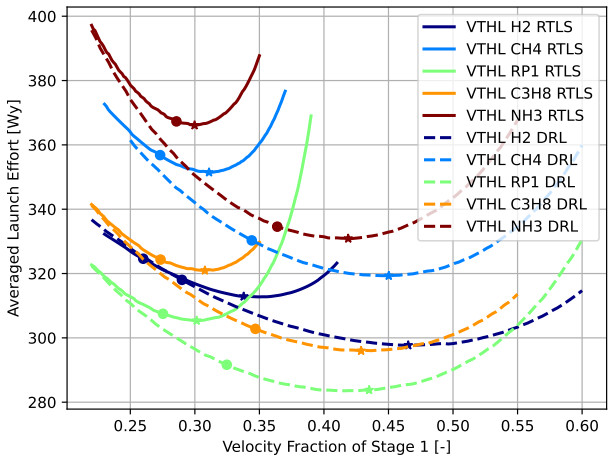

Figure 15: Launch costs vs. first stage ascent velocity fraction for kerosene, methane and hydrogen VTHL TSTO DRL vehicles targeting LEO. The circled dot (•) shows the minimal total mass configuration, while the asterix (∗) the minimal effort configuration.

Table 4: Results for VTHL launchers with cost optimal staging targeting LEO

Propellant		Hydrolox		Methalox		Kerolox		Propalox		Ammolox	
Recovery Type		RTLS	DRL	RTLS	DRL	RTLS	DRL	RTLS	DRL	RTLS	DRL
Stage 1	m_T [Mg]	305	373	582	650	596	670	585	637	832	857
	m_d [Mg]	40	49	52	58	49	55	50	55	69	71
	$m_{p,a}$ [Mg]	255	321	502	587	523	609	509	577	725	778
	$m_{p,r}$ [Mg]	7		23		19		21		30	
	SI [-]	0.15	0.15	0.10	0.10	0.09	0.09	0.09	0.09	0.09	0.09
	l [m]	57	61	54	56	50	52	52	53	59	59
	ΔV_a [km/s]	3.33	4.58	3.06	4.43	2.97	4.28	3.03	4.22	2.95	4.13
	ΔV_r [km/s]	0.57		1.06		0.92		0.97		0.96	
	$f_{\Delta V}$ [-]	0.34	0.47	0.31	0.45	0.30	0.43	0.31	0.43	0.30	0.42
	d_{drl} [km]		589		773		676		738		738
Stage 2	m_T [Mg]	126	76	219	115	240	128	227	129	307	163
	m_d [Mg]	10	7	12	7	12	7	12	7	15	9
	$m_{p,a}$ [Mg]	114	68	204	106	225	119	211	119	287	152
	$m_{p,r}$ [Mg]	1	1	1	1	1	1	1	1	2	1
	SI [-]	0.09	0.10	0.06	0.06	0.05	0.06	0.06	0.06	0.05	0.06
	l [m]	33	22	29	18	28	18	28	19	31	20
	ΔV_a [km/s]	6.52	5.27	6.79	5.42	6.88	5.57	6.82	5.63	6.90	5.72
	ΔV_d [km/s]	0.30	0.30	0.30	0.30	0.30	0.30	0.30	0.30	0.30	0.30
Launcher	m_T [Mg]	456	475	828	792	862	824	838	792	1166	1048
	$m_{L,ELV}$ [Mg]	22	20	23	20	22	20	22	20	22	20
	C_T [Wyr]	313	298	351	319	305	284	321	296	366	331
	l [m]	101	94	94	85	90	81	91	83	101	91
	d [m]	5.7	6.1	5.4	5.6	5.0	5.2	5.2	5.3	5.9	5.9

which could lead to larger structural reinforcements and considerable thermal protection. No simplified semi-empirical method could be derived to predict these conditions, and hence its feasibility is not guaranteed. Results for RTLS and DRL without additional propulsive manoeuvres are shown in Figures 14 to 19 and in Table 4.

The results show that kerosene, hydrogen and propane based launchers have certain advantages for these applications in terms of estimated effort, while methane and ammonia-based launchers obtain similar results (the later one performing worse for GTO). For the hydrogen configuration a lower total mass sensitivity with staging is also observed

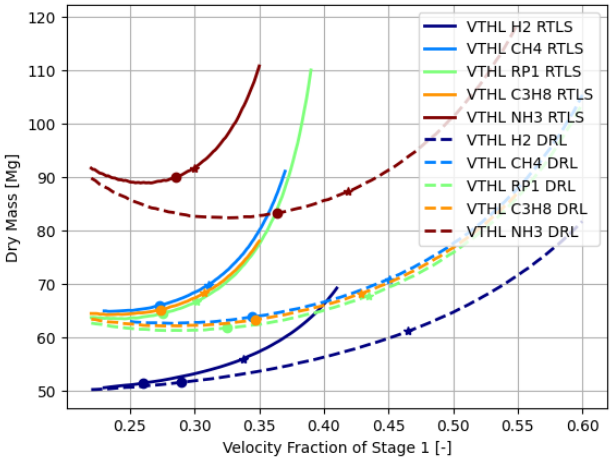

Figure 16: Total dry mass vs. first stage ascent velocity fraction for kerosene, methane and hydrogen VTHL TSTO vehicles targeting LEO. The circled dot (•) shows the minimal total mass configuration, while the asterix (∗) the minimal effort configuration.

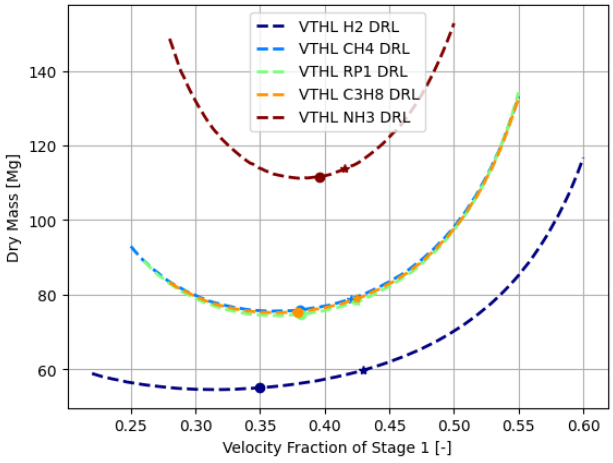

Figure 17: Total dry mass vs. first stage ascent velocity fraction for kerosene, methane and hydrogen VTHL TSTO vehicles targeting GTO. The circled dot (•) shows the minimal total mass configuration, while the asterix (∗) the minimal effort configuration.

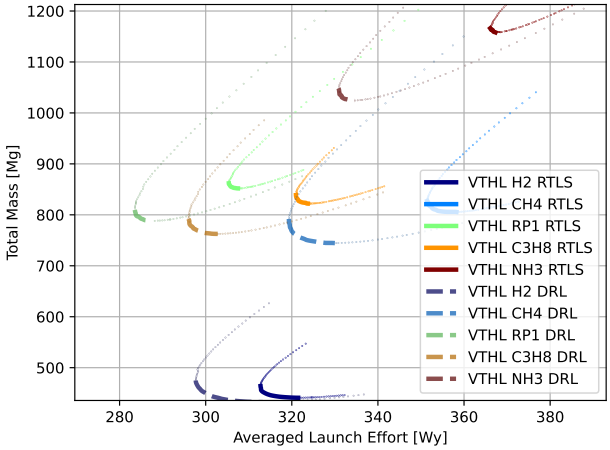

Figure 18: Total take-off mass vs. launch costs for kerosene, methane and hydrogen VTHL TSTO vehicles targeting LEO.

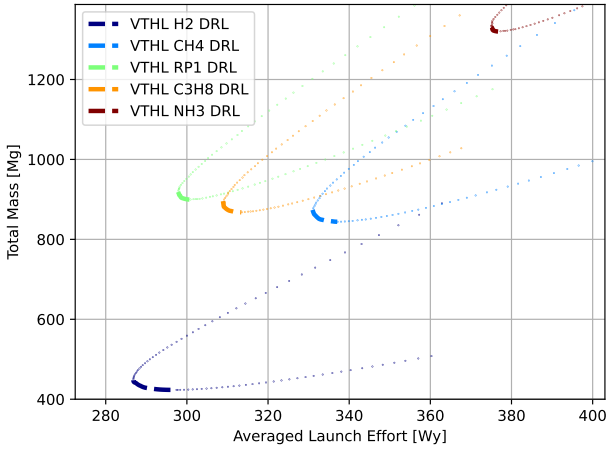

Figure 19: Total take-off mass vs. launch costs for kerosene, methane and hydrogen VTHL TSTO DRL vehicles targeting GTO.

in Figure 15 which might indicate a higher robustness and flexibility, partly why high staging values are derived by the algorithm to minimize launch effort. It also shows a lower launch effort performance than kerosene launchers when designed for GTO. In addition, the larger dry masses for the hydrocarbon and ammonia based launchers can lead to complicated recoveries if landing sites are unavailable and IAC approaches become necessary when considering towing limitations. Significant differences were also observed between the hydrogen-based launchers in terms of stage size between minimal effort and take off mass configurations, where the later one could lead to around 10% higher effort at the expense of larger total mass.

It is also interesting to see that the TRANSCOST model predicts significantly larger costs for the VTHL configurations compared to the VTVL stages, as seen in Figure 10 and Figure 18, even though the dry masses are similar. Although this can provide valuable in-sights, it has to be noted that the model is based on historical vehicles or concepts, and no VTHL vehicles have ever flown. This is mostly caused by the CER from the TRANSCOST model in which the mass specific production effort is estimated to be significantly higher than for VTVL stages (which are treated as equivalent to ELV stages). Also, in both cases the same number of reuses as well as the same assumption for refurishment effort is used, while in practice the different approaches will differ in that regard. So the comparison between different resuable types is subject to large uncertantities and caveats. The cost estimation model also contains various parameters which can be considerably different for each architecture depending on the know-how of the workforce at various stages and other factors, and the productivity factor from the historical figures may have increased significantly in the last decades with the rise of new cost engineering strategies.[37] Therefore, it is not possible to obtain definite cost effectiveness conclusions from the relative differences between the configurations and careful engineering judgment is necessary.

5. Conclusions

This study introduced a fast optimal staging methodology to assess different reusable launch vehicle architecture options at early conceptual design stages, which was applied to assess the differences in kerosene, propane, ammonia, methane and hydrogen based reusable launchers with VTVL and VTHL technology. The assessment shows that VTVL and VTHL technology has significant benefits in terms of possible launch effort compared to purely expendable launchers. In addition, hydrogen technology led to highly efficient launchers with significantly low total and a dry mass 12% lower than the hydrocarbon stages. These later ones showed similar total and dry masses, while the ammonia launcher had a 15% dry mass increase with respect to the later ones. In terms of launch effort, kerosene stages showed the least costs, although the margin difference with the hydrogen stage decreased in the VTVL case when optimizing for high energetic GTO missions, and reversed in the VTHL DRL case for GTO with hydrogen showing lower launch effort. Furthermore, it was assumed that all stages had similar engine weight ratio, while past studies showed that it is slightly lower for hydrogen as a result of its additional cryogenic insulation. Although this was partly accounted for in terms of total structural index through a calibration with historical data of expendable stages, it might underestimate effort for non-hydrogen stages as engines are weighted higher. As reduced performance was observed for RLVs in general flying to GTO missions, future studies could address the introduction of a third stage, specially for the ammolox combination

which suffered a larger penalty. Nevertheless, the cost metric depends considerably on the different assumptions used for its development, manufacturing and operations. It is still possible that heavier launchers could lead to significantly higher recovery, maintenance and refurbishment costs because of handling and transportation difficulties or lower robustness against mass budget growth during development. The staging was optimized for both minimal total mass as well as minimal total cost and substantial differences were found in the result launcher sizing, especially for the RLV architectures. The cost optimized launchers exhibited significantly larger first stages, with the staging velocity being up to 1 km/s shifted in comparison to the result for minimal total mass. Nevertheless, given the low fidelity of the used methods the results have to be used with careful engineering judgment. The CER estimates for methane, propane and ammonia based stages use a linear interpolation with average mass based propellant storage temperatures between those for kerosene and hydrogen, assumed analogous to linear cost growth with cryogenic handling, and cannot be validated with historical data. A caloric averaged temperature would have resulted in significant lower costs for ammolox. Moreover the algorithm is known for overestimating the size of the upper stage, might underestimate recovery velocity budgets from the observed separation conditions, and neglects sizing influences on the aerodynamic forces except for ballistic coefficient dependencies in the final aerodynamic falls during recovery of the VTVL stages. Despite this, the preceding analysis and methodology strategy showed advantages in terms of its fast and flexible applicability, and can be used to initialize further detailed system and trajectory assessments.

6. Acknowledgments

The authors would like to thank Dr. Aaron Koch for his valuable insights on the staging optimization algorithms, and the ASCenSIon (Advancing Space Access Capabilities - Reusability and Multiple Satellite Injection) network. The project leading to this application has received funding from the European Union's Horizon 2020 research and innovation programme under the Marie Skodowska-Curie grant agreement No 860956.

References

[1] M. Vertregt. Calculation of Step-Rockets. *Journal of the British Interplanetary Society*, 14:20–25, 1955.

[2] Schurmann, Ernest E. H. Optimum Staging Technique for Multistaged Rocket Vehicles. *Journal of Jet Propulsion*, 27(8):863–865, 1957.

[3] H. H. Hall and E. D. Zambelli. On the Optimization of Multistage Rockets. *Journal of Jet Propulsion*, 28(7):463–465, 1958.

[4] Ulrich Walter. *Astronautics: The physics of space flight*. Third edition edition, 2019.

[5] J. S. Gray and R. V. Alexander. Cost and weight optimization for multistage rockets. *Journal of Spacecraft and Rockets*, 2(1):80–86, 1965.

[6] Richard J. Weber. Technical Comment: Optimization of Multistage Rockets. *ARS Journal*, 31(6):848–851, 1961.

[7] R. L. Chase. Multistage rocket staging optimization. *Advances in Astronautical Science*, 6:621–629, 1961.

[8] John S. MacKay and Richard J. Weber. Performance Charts for Multistage Rocket Boosters. Technical report, National Aeronautics and Space Administration, 1961.

[9] Edgar R. Cobb. Optimum Staging Technique to Maximize Payload Total Energy. *ARS Journal*, 31(3):342–344, 1961.

[10] Charles N. Adkins. Optimization of multistage rockets including drag. *Journal of Spacecraft and Rockets*, 7(6):751–755, 1970.

[11] Ronald W. Humble, Gary N. Henry, and Wiley J. Larson. *Space propulsion analysis and design*. Space technology series. McGraw-Hill, New York, 1st revised ed. edition, 2007.

[12] Angella Trulove and Kevin Whitaker. Rocket stage optimization using a simple genetic algorithm. In *29th Joint Propulsion Conference and Exhibit*, 1993.

[13] Rizwan Ullah, De-Qun Zhou, Peng Zhou, Mukarrum Hussain, and M. Amjad Sohail. An approach for space launch vehicle conceptual design and multi-attribute evaluation. *Aerospace Science and Technology*, 25(1):65–74, 2013.

[14] Rizwan Ullah, De Qun Zhou, Peng Zhou, and Majid Baseer. A novel weight allocation and decision making method for space launch vehicle design concept selection. *International Journal of Industrial and Systems Engineering*, 19(2):155, 2015.

[15] Walter E. Hammond. *Design Methodologies for Space Transportation Systems*. American Institute of Aeronautics and Astronautics, Reston ,VA, 2001.

[16] Francesco Castellini, Michèle R. Lavagna, Annalisa Riccardi, and Christof Büskens. Quantitative Assessment of Multidisciplinary Design Models for Expendable Launch Vehicles. *Journal of Spacecraft and Rockets*, 51(1):343–359, 2014.

[17] Francesco Castellini and Michèle R. Lavagna. Comparative Analysis of Global Techniques for Performance and Design Optimization of Launchers. *Journal of Spacecraft and Rockets*, 49(2):274–285, 2012.

[18] Reza Jamilnia and Abolghasem Naghash. Simultaneous optimization of staging and trajectory of launch vehicles using two different approaches. *Aerospace Science and Technology*, 23(1):85–92, 2012.

[19] Ezgi Civek-Coskun and Kemal Özgören. Space Launch Vehicle Design with Simultaneous Optimization of Thrust Profile and Trajectory. In *AIAA SPACE and Astronautics Forum and Exposition*, 2017.

[20] Aaron D. Koch. Optimal staging of serially staged rockets with velocity losses and fairing separation. *Aerospace Science and Technology*, 88:65–72, 2019.

[21] Kai Dresia, Simon Jentzsch, Günther Waxenegger-Wilfing, Robson Dos Santos Hahn, Jan Deeken, Michael Oschwald, and Fabio Mota. Multidisciplinary Design Optimization of Reusable Launch Vehicles for Different Propellants and Objectives. *Journal of Spacecraft and Rockets*, pages 1–13, 2021.

[22] Matthew T. Vernacchia and Kelly J. Mathesius. Strategies for Reuse of Launch Vehicle First Stages. In *69th International Astronautical Congress IAC*, 2018.

[23] Nguyen X. Vinh. *Hypersonic and planetary entry flight mechanics*. Michigan U.P, Ann Arbor, 1980.

[24] H. Wittenberg. Lecture Notes AE4-870A: Rocket Motion. Technical report, 2016.

[25] Andrew B. Lambe and Martins, Joaquim R. R. A. Extensions to the design structure matrix for the description of multidisciplinary design, analysis, and optimization processes. *Structural and Multidisciplinary Optimization*, 46(2):273–284, 2012.

[26] Guillermo J. Dominguez Calabuig, Loïs Miraux, Andrew Ross Wilson, and Alberto Sarritzu. Eco-design of future reusable launchers: insight into their life-cycle and atmospheric impact. In *9th European Conference for Aeronautics and Space Sciences (EUCASS)*, 2022.

[27] A. Valera-Medina, H. Xiao, M. Owen-Jones, W.I.F. David, and P. J. Bowen. Ammonia for power. *Progress in Energy and Combustion Science*, 69:63–102, 2018.

[28] S. Gordon and Mc Bride, B. J. Computer Program for Calculation of Complex Chemical Equilibrium Compositions and Applications - Volume I Analysis and Volume II Users Manual and Program Description. Technical report, 1958.

[29] Sven Stappert, Jascha Wilken, and M. Sippel. Evaluation of European Reusable VTVL Booster Stages. In *AIAA SPACE and Astronautics Forum and Exposition*, 2018.

[30] Justin S. Gray, John T. Hwang, Martins, Joaquim R. R. A., Kenneth T. Moore, and Bret A. Naylor. OpenMDAO: an open-source framework for multidisciplinary design, analysis, and optimization. *Structural and Multidisciplinary Optimization*, 59(4):1075–1104, 2019.

[31] D. R. Chapman. An approximate analytical method for studying entry into planetary atmospheres. Technical report, Washington D.C., 1958.

[32] Pirooz Mohazzabi and James H. Shea. High–altitude free fall. *American Journal of Physics*, 64(10):1242–1246, 1996.

[33] Jan Benacka. High-altitude free fall revised. *American Journal of Physics*, 78(6):616–619, 2010.

[34] Dietrich E. Koelle. TRANSCOST Statistical-Analytical Model for Cost Estimation and Economic Optimization of Space Transportation Systems. Technical report, TCS-Trans Cost Systems, Ottobrunn, Germany, 1991.

[35] Guillermo J. Dominguez Calabuig. Conceptual Cost Estimation for Recovery and Refurbishment Operations of Reusable Launch Vehicles. Technical report, 2019.

[36] Sven Stappert, Jascha Wilken, L. Bussler, and Martin Sippel. A Systematic Comparison of Reusable First Stage Return Options. In *8th European Conference for Aeronautics and Space Sciences (EUCASS)*, 2019.

[37] Sven Stappert, Jascha Wilken, and Martin Sippel. Evaluation of Parametric Cost Estimation in the Preliminary Design Phase of Reusable Launch Vehicles. In *9th European Conference for Aeronautics and Space Sciences (EUCASS)*, 2022.